SEMARAK ILMU PUBLISHING

Journal of Advanced Research in Fluid Mechanics and Thermal Sciences

Journal homepage:
https://semarakilmu.com.my/journals/index.php/fluid_mechanics_thermal_sciences/index
ISSN: 2289-7879

Turbulent Fluid Flow and Heat Transfer Enhancement Using Novel Vortex Generator

Bassam Amer Abdulameer Shlash[1,2,*], Ibrahim Koç[1]

[1] School of Engineering and Architecture, Altinbas University, Istanbul, Turkey
[2] Federal Board of Supreme Audit Editorial, Baghdad, Iraq

ARTICLE INFO

Article history:
Received 6 February 2022
Received in revised form 5 May 2022
Accepted 11 May 2022
Available online 7 June 2022

Keywords:
Turbulent flow; vortex generator; heat transfer; Nusselt number; skin friction coefficient

ABSTRACT

One of several effective methods for improving heat transfer in heat exchangers is the use of vortex generators in channels. The flow of fluid through a channel with a vortex generator is disrupted by the development of recirculation zones on the step wall, which improves fluid mixing and heat transmission. The current work investigates the flow and heat transfer of turbulent fluid flow through channels with various vortex generator designs mathematically (triangular, half-circle, and quarter circle). The finite volume method (FVM) is used to discretize and solve the continuity, momentum, and energy equations. The SIMPLE algorithm approach is used to connect the pressure and velocity fields within the domain. The effect of geometrical factors such as step height (2, 3, 4, 5, and 6 mm) on the flow and heat fields is demonstrated and analyzed, as is the effect of Reynolds number. As the step height increases, so do the surface Nusselt number and skin friction coefficient, which peak at 4 mm. According to the findings, as Re increases, so does the average Nusselt number. The quarter circle vortex generator has the best thermal-hydraulic performance at a 4 mm amplitude height, followed by the triangle vortex generator. The simulation results are consistent with those found in the literature.

1. Introduction

Many industries use compact heat exchangers, like aerospace, chemical engineering, geothermal, process plant, power grid, cooling system, Ventilation tank. The blades of the internally cooled gas turbine in addition to the solar collector which is cooled by air and cooling the electronic chip in addition to the chemical mixer, sewage collector, car radiator, nuclear reactor cores and many other engineering applications. In such systems, an effective heat exchanger might result in less energy usage, which would be beneficial to both the economy and the environment. Heat exchanger performance is increasingly being demanded for reasons of compactness, cost-effective production and operation, energy saving, and even environmental concerns. The importance of these challenges has prompted further research into heat transfer augmentation strategies [1-3].

* *Corresponding author.*
E-mail address: shlash.bassam@yahoo.com

https://doi.org/10.37934/arfmts.96.1.3652

Tiny flow turbulators or protrusions punched in the boundary layer, such as wings and winglets configurations, can be used to create streamwise vortices. Longitudinal and transverse vortices are created by VGs. Heat transfer enhancement is more efficient with longitudinal vortices than with transverse vortices. Although the thermal system's thermal performance can be archived, It can be observed that there is a penalty for pressure drop, and therefore the wings were used effectively and for the aim of improving heat transfer in the modern thermal structure, the reason for this is because it may generate a longitudinal vortex that cuts the main flow in addition to reducing pressure loss [4-6].

In recent decades, there has been a great deal of interest in the properties of fluid flow and heat transfer in flow channels. Several of these applications use gases as the heat transfer medium rather than liquids. By definition, the heat transmission rate of gases is lower than that of liquids. As a result, heat transfer augmentation methods that increase heat transfer rates are particularly appealing. Several previous researchers conducted experimental and numerical analyses of heat transfer augmentation methods. As the industrial world has advanced, many academics have become interested in reducing the volume of heat exchangers and improving their heat transfer performance. High-performance thermal systems are required due to the increased pressure drop associated with increased heat transmission. Reduce the underlay thermal resistance near the wall, which is the point where the viscous impacts of the underlayer are most visible, to improve the coefficient of heat transfer. This is completed by increasing the instability of the main fluid flow, allowing turbulent eddies to penetrate deeper into this layer. Thermal resistance can be reduced and heat transfer improved by using VG that is perforated or linked to the channel wall's inner surface. The VG is a type of extended surface that is made by stamping or punching from the fin. VG not only disrupts the formation of the flow field and boundary layer, but also swirls the fluid, resulting in significant core and wall fluid exchange as well as increased heat transfer between the channel walls and flowing fluid. Vortex generators of various types are used in heat sinks, circular and non-circular channels, tube-fin heat exchangers, mini and micro-channels, flat-plate-fin heat exchangers, and other engineering applications [7-10]. Chang *et al.,* [10] used VG to create longitudinal vortices in the main flow path of a tube bank heat exchanger to improve heat transmission on the fin surface. According to Hermon *et al.,* [11], the size, length, and location of delta winglets from the wall, two vortices can allow to rotate in reverse by passing through the bottom wall while there is flow both towards and away from the wall. This complex phenomenon of unstable flow improves heat transfer in addition to pressure and expansion of the underlying boundary layers.

The thermal performance of heat exchangers is significantly affected by vortex generators. VG's type, geometry, and angle of attack affect this effect. These parameters are discussed with details as following. Winglets perform better than wings in terms of heat transmission, according to Li-Ting *et al.,* [12] a DWP achieves marginally superior to a rectangular-winglet pair. When compared to a plate, they observed that VG's DWP enhances heat transmission by 46 % at Re = 2000 and 120 % at Re = 8000. Their study reveals that the greatest heat transmission of the RWP of the VG case occurs at $45o \leq \beta \leq 65o$, which is lower than the DWP of the VG case. A substantial reduction in the Nu number was noticed at $\beta = 90o$. When VGs are utilized, the friction coefficient increases marginally. In terms of compactness criterion, Ferrouillat *et al.,* [13] demonstrated that the DWP was more efficient than the RWP for many turbulent models used.

When RWP of VGs was utilised, Sanders and Thole [14] found that heat transfer augmentations of up to 39 percent were achieved with corresponding friction factor increases of up to 23 percent. Guobing and Qiuling [15] investigated a new vortex generator VG form for the curved trapezoidal winglet pair (CTWP) and compared it to standard vortex generators such as RWP, trapezoidal winglet, and DWP. According to the researchers, DWP worked best in laminar and intermediate flow zones,

whereas CTWP excelled in completely turbulent flow. The overall average heat transmission coefficient using DW of vortex generators was 75 percent greater than a plain fin-flat tube heat exchanger and 45 percent higher than a plain fin-circular tube heat exchanger, according to Yoo *et al.,* [16].

Sun *et al.,* [17] looked into the turbulent thermal-hydraulic behavior of circular heat exchanger tubes using a large number of rectangular winglet vortex generators. The impact of geometric parameters such as ratio of the height (HR = 0.05, 0.1, 0.2), Number of circumferential of rectangular winglets (N = 4, 6, 8), and pitch ratio (PR = 1.57, 3.14, 4.71) are investigated. The friction factor and Nu are increasing with the height and number of rectangular winglets based on results because of enhanced fluid mixing performance caused by multi-longitudinal vortices with increased turbulent kinetic energy. The friction factor and Nu ratios for the Reynolds numbers studied are 1.46–11.63 and 1.15–2.32, respectively. When the height ratio is 0.05, the TEF improves as the number of rectangular winglets rises, while the opposites is true in the other situations. The TEF can reach 1.27.

Furthermore, correlations for the Nu and friction factor are constructed for practical applications based on the experimental results Jiao *et al.,* [18]. The numerical research of the performance of heat transfer and the dynamics of flows in channels by using a miniature cubic vortex generator (MCVGs), note that the MCVGs are completely immersed inside viscous sub-layers and within the heat transfer region and the logarithmic law area. Here, the researcher shows us by examining the effect of MCVGs on the structure The turbulent coherent is at a finely different location. Hence, the success was fully verified aimed at the improvement of heat transmission by the joint performance metric. In the viscous sublayer, the overall performance parameter of MCVGs is less than 1. Furthermore, using MCVGs, the transition area obtains the highest combined performance parameter. Furthermore, the friction coefficient lowers to 8.05 percent when compared to a rectangular channel without MCVGs, but the Nusselt number Nu climbs to 5.17 percent. At the same time, the total performance metric rises by 8.15 percent.

According to Althaher *et al.,* [19]. The friction factor and Nu number are related to the size of the VG's DWP. The VG's geometry had a big impact on the Nu number, but it only had a minor impact on the friction factor. In 2012, Ahmed *et al.,* [20]. found that combining both VG and SiO2–EG nanofluids improved rate of heat transfer. The Nu avg number increased by 50.0 percent when the Reynolds number was raised from 100 to 800.

In recent years, Carpio and Valencia [21] have computed thermal efficiency in the range 9 alternating, 18 alternating, 18 aligned, 27 alternating and 39 alternating LVG for a low-intensity heat exchange using flat tubes in a laminar regime. Delta winglets with a 35-° angle of attack were built of vortex generators. Each shape has been determined by the local heat flow and global friction factor and Nu. The figures from Re ranged from 400 to 2000.

Zhang *et al.,* [22] investigated the flow dynamics and heat transfer of VG in a rectangular ribbed channel with a great aspect ratio and Re varied from 20000 to 100000. All Reynolds numbers, Winglet VGs combined with a common flow design provide the best overall thermal efficiency in most situations. The flow characteristics also show that longitudinal VGs can make vortices in the boundary layers improving flow mixing and heat transfer efficiency.

Moosavi and colleagues [23] The three-dimensional heat transfer was quantitatively studied using transverse VG vortex generators and the porous medium, and the low flow pressure of the fluid was observed in the interior of the micro-channel. A total of 14 cases were then thoroughly examined, each with a different type of VG, semi-porous, or fully porous content. According to the mathematical results, heat transfer by convection increases with increasing transverse VG. The heat transfer coefficient of a fully filled porous medium is 12 times that of an empty microchannel, whereas the heat transfer coefficient of an eight VG with 12.5 percent channel height is 2.6 times that of an empty

microchannel, and when attempting to achieve a high heat coefficient, the liquid flow pressure drop increases frequently. The thermal efficiency ratio is calculated to regularize the change in pressure, drop, and heat coefficient. According to Zhang *et al.,* [24], the microchannel containing VG and the bottom- and top-injected porous medium has the highest thermal efficiency at both high and low Re. According to a review of the literature, the equilateral triangular conduit has a lower heat lower pressure and transfer rate than other types of triangular conduit within a similar boundary condition, and note the use of a passive technique that contains pairs of vortex generators in a variety of applications. This is due to the change in heat transmission that occurs as pressure decreases. In comparison to the other four traditional vortex generator VG designs, the Delta Wing Pair (DWP) improves heat transmission and reduces pressure loss. Furthermore, when compared to the entire surface of the heat transfer, the VG protrusion area is extremely small. As a result, the current study aims to investigate the effect of various vortex generator designs on fluid flow and heat transfer. Furthermore, the study will take into account the effect of VG step height.

Due to increase of energy demands in recent decades, much effort has been put into studying and improving heat exchanger thermal efficiency. The goal of this research is to determine the heat enhancement levels that can be achieved in a smooth channel by instilling VG positioned on the bottom wall. No experimental or numerical research of the effect of installing a vortex generator VG (half circle and quarter circle design) in a channel has been done, as indicated in previous works [6-8]. Furthermore, no investigation on the impact of VG step height on the (Nu) and skin friction coefficient has been conducted.

2. Assumptions and Physical Model

Figure 1 depicts the flow structure and geometry used in this analysis. The duct has an upper and lower wall. Under continuous heat flux conditions, the lower surface is heated. In the computations the height of the duct (H = 10 mm) is used as a feature. The duct length is 10 times the intake height (L/H = 10). The rib lies downstream of the leading lip of the conduit (X/H = 2). The step height of the vortex generator VG is 2, 3, 4, 5, and 6 mm, and the length of the vortex generator VG is 8 mm. The working fluid enters the duct at T_{in} and leaves at T_{out}, both at constant temperatures. The heat flux applied to the area following the VG in order to look into the influence of the vortex on fluid flow and heat transfer. Table 1 present the value of the geometry dimensions.

Table 1
The value of geometry dimensions

Parameters	Value (mm)
L_1	50
L_2 (Pitch diameter)	20
L_3	70
S	2, 3, 4, 5, and 6
H	10

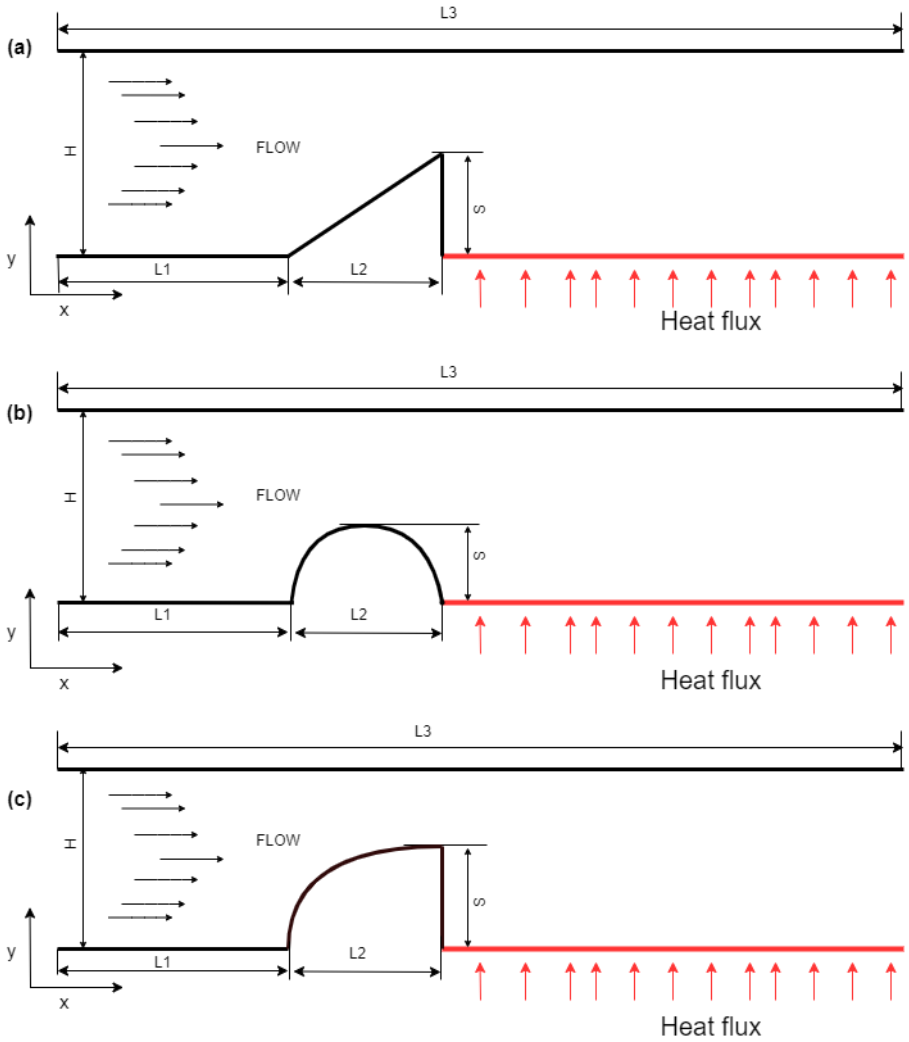

Fig. 1. Schematic diagram of the channels combined with: (a) Triangular VG, (b) half circler VG, (c) quarter circler

2.1 Boundary Conditions

The limits for the 2D channel flow are determined by computer domain. The inlet and outlet limits of a duct on the x-y plane. At 300 K, the fluid inlet temperature is called uniform. A constant thermal flux border (q = 500 W/m2) is specified for the lower wall. Ribs are believed to be adiabatic. At the duct's inlet, uniform velocity is assumed, and the Re ranges from 5000 to 20000. The inlet fluid velocity is calculated as follows

$$u_{in} = \frac{Re\,\mu}{\rho\,H} \tag{1}$$

where H the channel's height for the outlet boundary condition, a default boundary condition including zero-gradient conditions has been used. The Re is the Reynolds number, μ viscosity and ρ density.

2.2 Governing Equations

The fluid energy equations, continuity and momentum of RANS were determined by the k-ε RNG model. The parameters were stable-state flow and Newtonian, incompressible fluid, 2 dimensions and continuous flow. Said *et al.,* [25]. described how the controlling equations should be constructed. The continuity equation

$$\frac{\partial(\rho\bar{u})}{\partial x}+\frac{\partial(\rho\bar{v})}{\partial y}=0 \tag{2}$$

The x-Momentum equation

$$\frac{\partial}{\partial x}(\rho\bar{u}\bar{u})+\frac{\partial}{\partial y}(\rho\bar{u}\bar{v})=-\frac{\partial P}{\partial x}+\frac{\partial}{\partial x}\left[(\mu+\mu_t)\frac{\partial\bar{u}}{\partial x}\right]+\frac{\partial}{\partial y}\left[(\mu+\mu_t)\frac{\partial\bar{u}}{\partial y}\right] \tag{3}$$

The y- Momentum equation

$$\frac{\partial}{\partial x}(\rho\bar{u}\bar{v})+\frac{\partial}{\partial y}(\rho\bar{v}\bar{v})=-\frac{\partial P}{\partial X}+\frac{\partial}{\partial X}\left[(\mu+\mu_t)\frac{\partial\bar{v}}{\partial X}\right]+\frac{\partial}{\partial y}\left[(\mu+\mu_t)\frac{\partial\bar{v}}{\partial y}-\frac{2}{3}\rho\frac{\partial k}{\partial y}\right] \tag{4}$$

The conservation of energy equation

$$\frac{\partial}{\partial x}(\rho\bar{u}T)+\frac{\partial}{\partial y}(\rho\bar{v}T)=\frac{\partial}{\partial x}\left[\left(\frac{k}{C_P}+\frac{\mu_t}{Pr_t}\right)\frac{\partial T}{\partial x}\right]+\frac{\partial}{\partial y}\left[\left(\frac{k}{C_P}+\frac{\mu_t}{Pr_t}\right)\frac{\partial T}{\partial y}\right] \tag{5}$$

where μ_t represents the turbulent dynamic viscosity, ρ is the Density, k Thermal conductivity, $\bar{V}$ velocity vector, ū Velocity vector, T temperature, K, Prt Turbulent Prandtl number, CP Specific heat capacity, ε Emissivity, f Friction factor. This is proportional to k and can be considered using the following formula

$$\mu_t=\rho C_\mu f_\mu\left(\frac{k^2}{\varepsilon}\right) \tag{6}$$

2.3 Method of Solution

The regulating equations with related limits have already been resolved by (FVM) in the Ansys-Fluent V19 commercial CFD program. The flow sector was solved using the SIMPLE algorithm, and the convection standings were calculated using a second-order upwind differencing scheme. The k-ε turbulent model with RNG was chosen because it is appropriate for the separation flow [24] and the second-order upwind gap approached the diffusion term in the momentum and energy equations. The grid has been changed to the lower wall and step to measure the velocity gradient. For both the energy and velocity components, the scaled residual was set to 10^{-6}.

2.3.1 Grid study and code validation

The meshing tool ANSYS V.19 was the basis for the grids used in this research. For the numerical domain, a standardized and non-uniform grid is used. As the velocity components and the temperature of the flow differ significantly, a fine grid is placed in both the septic region and the downstream wall of the channel. To test the influence of grid sizes on the calculated values, four

separate grids were analyzed, as presented in Table 2. The relative error percentage between the fourth and third grids has been found to be 0.0085% and can be ignored. In the current investigation, a grid of 378,000 is therefore chosen to decrease effort and calculation period. The measurement of error is calculated as

$$e\% = \left|\frac{Q-Q_{n-1}}{Q_{n-1}}\right| \tag{7}$$

where Q represents any quantity.

Table 2
Grid independent study

Grid No.	Grid nodes	Nu	e %	$u\ (ms^{-1})$	e %	y^+	T (K)	e %
1	98,000	169.354	—	0.5621	—	0.6231	300.0811	-
2	138,000	170.928	2.446	0.5632	0.306	0.6245	300.0821	0.302
3	214,000	171.546	2.445	0.5655	0.334	0.7489	300.0830	0.312
4	378,000	171.921	0.085	0.5656	0.079	0.7138	300.0831	0.001

Code validation was performed by comparing Hamdi *et al.,* [6]. data. The average Nusselt number Nu and the coefficient of skin friction are consistent as showed in Figure 2.

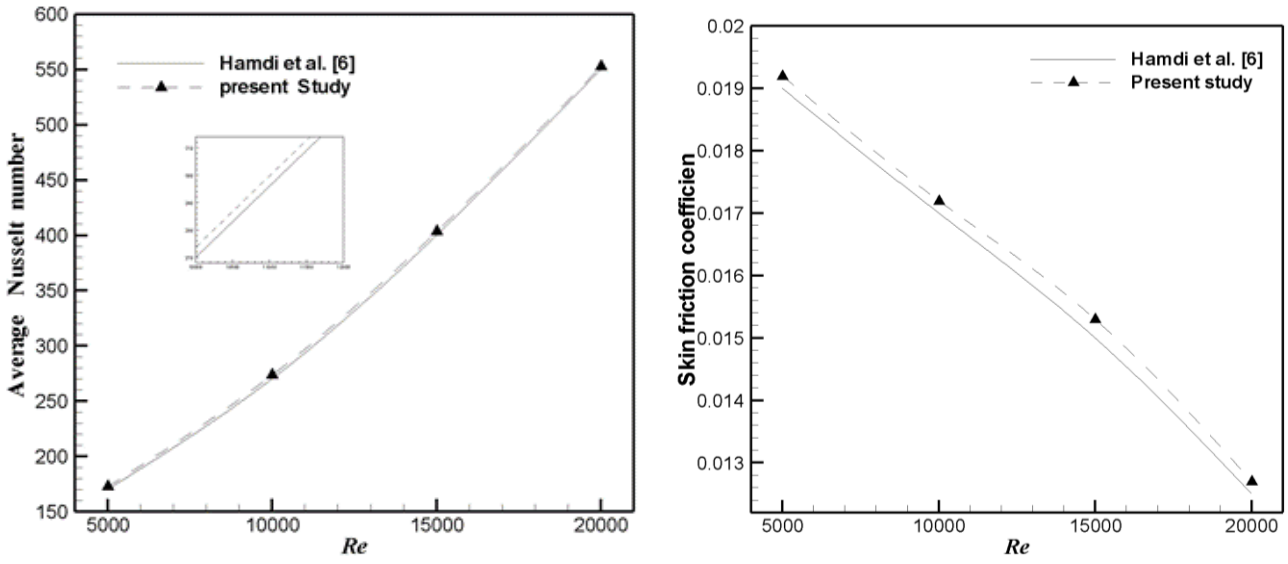

(a) (b)

Fig. 2. Validation of the present CFD results for pure water with numerical data from previous studies: (a) average Nusselt number, (b) Skin friction coefficient

3. Results and Discussion

This chapter shows the numerical outcomes of the current research. The primary goal of this numerical analysis is to examine the turbulent flow and heat transfer through a channel coupled with a separate VG such as triangular, half circle, and quarter circle for Re ranging from 5,000 to 20,000, step height (2, 3, 4, 5, and 6 mm), and fixed pitch diameter which is 20 mm.

The arithmetical results of forced convective fluid flow and heat transfer over channel combined with different VG are described in the first part of the analysis. This section presents and interprets the effects of Re and VG shape on hydraulic and thermal efficiency. The findings of this analysis corroborate previous findings by Ahmad *et al.,* [24] and Boonloi *et al.,* [1].

3.1 Effect of Different Vortex Generator Shapes

The installation of vortex generators in the channels greatly affects the fluid flows and heat transfer, and can notice this in Figure 3 (a, b), and it is also possible to observe the Nusselt Number (Nu) for the surfaces in addition to the skin friction coefficient inside the channels and along the bottom wall at Re = 5000 and height = 5 mm. The Nu for the quarter circle VG was found to be the largest as compared to the other shapes, The Nusselt number for the triangular VG, on the other hand, was determined to be the lowest. In comparison, the skin friction coefficient for the half circle VG is the lowest, followed by the quarter circle VG and the triangular VG.

Figure 3(a) reveals that the Nusselt number increases after each VG form phase compared to the straight channel. This is because the vortex generator produces a vortex, which improves the heat transmission ratio. The Nusselt number decrease occurs after the recirculation region, i.e., when the flow has completely formed.

The skin friction coefficient distributions for all VGs have the same frequency, as shown in Figure 3(b), with maximum and minimum values occurring exactly after the VG site. In addition to the flow after the VG created a higher recycle zone and a thin border layer. The quarter VG was therefore more effective, resulting in greater Nusselt number rates. At Re = 5,000 and step height = 5 mm, Figure 4 displays the impact of various VG shapes on the velocity distribution.

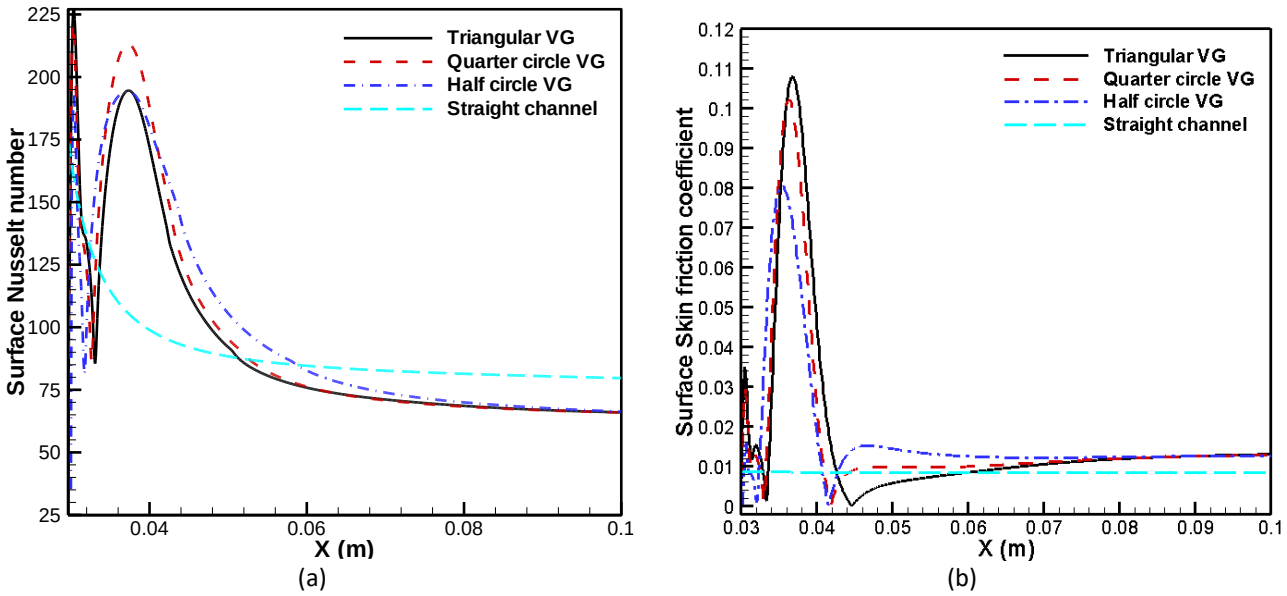

Fig. 3. The distribution of (a) surface Nusselt number and (b) Skin friction coefficient along the axial direction of the channel at various VG shapes and Re = 5,000

Figure 4 depicts the effects of different VG shapes on the velocity distribution at Re = 5,000 and phase height = 5 mm. The recirculation area was formed near the step's corner, which corresponds to the results of the fluid flow after the sudden expansion as showed in the literature [25], and [7]. The geometry of the VG was critical in determining the velocity streamline. Because of the sharp edge of the wall, a stable vortex was created after each VG shape step. As showed in Figure 4 the channel with the quarter circle has the greatest velocity gradient behind the step, Figure 4 (c) shows this. As the velocity gradient upsurges, the thermal boundary layer becomes thinner. The stresses are caused between the surface layer and the viscous sub-layer, causing the velocity to drop at the walls. The installation of VG in the channel, on the other hand, increases the distribution of velocity near the

wall, resulting in better combination of the flow layers. The minus velocity refers to the vortex (reverses flow) due to the sudden expression after the step.

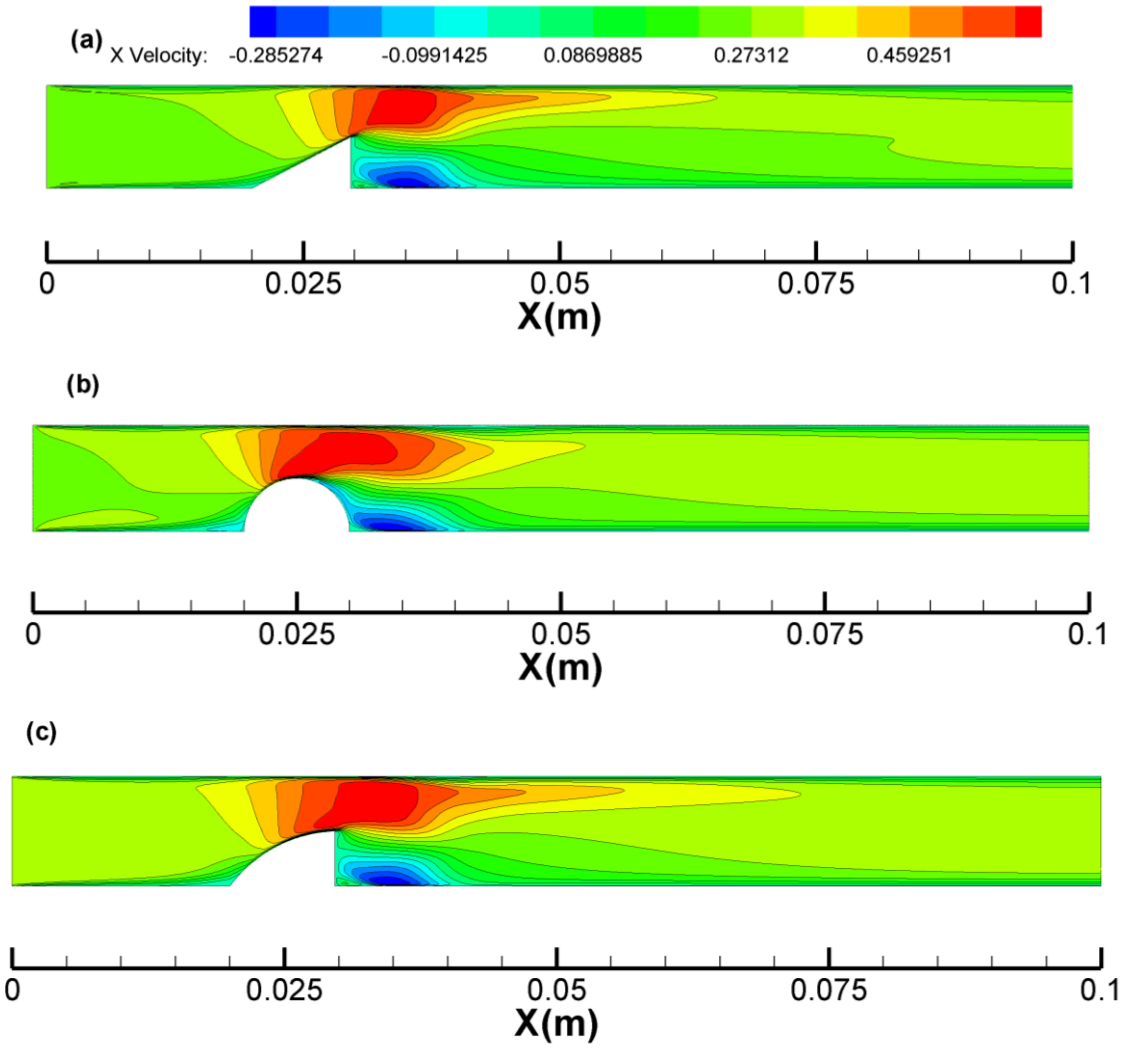

Fig. 4. Velocity streamlines through channel with insulation of (a) triangular VG, (b) Half circle VG, and (c) Quarter circle VG

Figure 5 present the Turbulence intensity at Re = 5,000 and a step height of 5 mm, through the channel with different VG shapes. The impact of various VG shapes on the turbulent intensity distribution is observed. The figure show that the channel with half circle and triangular vortex has the highest turbulence intensity. Moreover, there turbulence intensity of these two VG has almost the same pattern. The variations in turbulence intensity distribution are due to the influence of different vortex generator forms on the fluid flow.

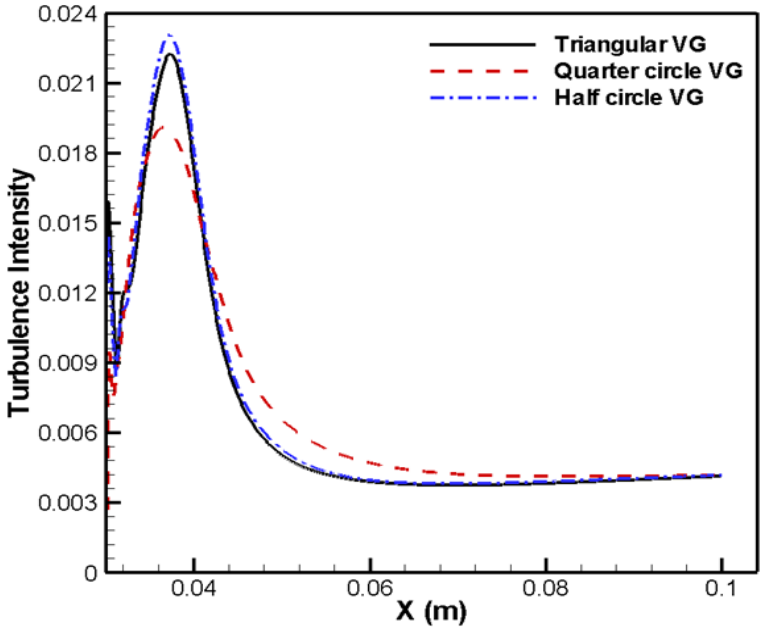

Fig. 5. Turbulence intensity through channel with insulation of (a) triangular VG, (b) Half circle VG, and (c) Quarter circle VG

Figure 6 show At Re = 5,000 and a step height of 5 mm, the impact of various VG shapes on the turbulent kinetic energy distribution. it is observed from the figure that the channel with half circle vortex has the highest turbulent kinetic energy rate followed with the quarter circle vortex the triangular vortex shape has the lowest turbulent kinetic energy. The variations in turbulent kinetic energy distribution are due to the influence of different vortex generator forms on the fluid flow.

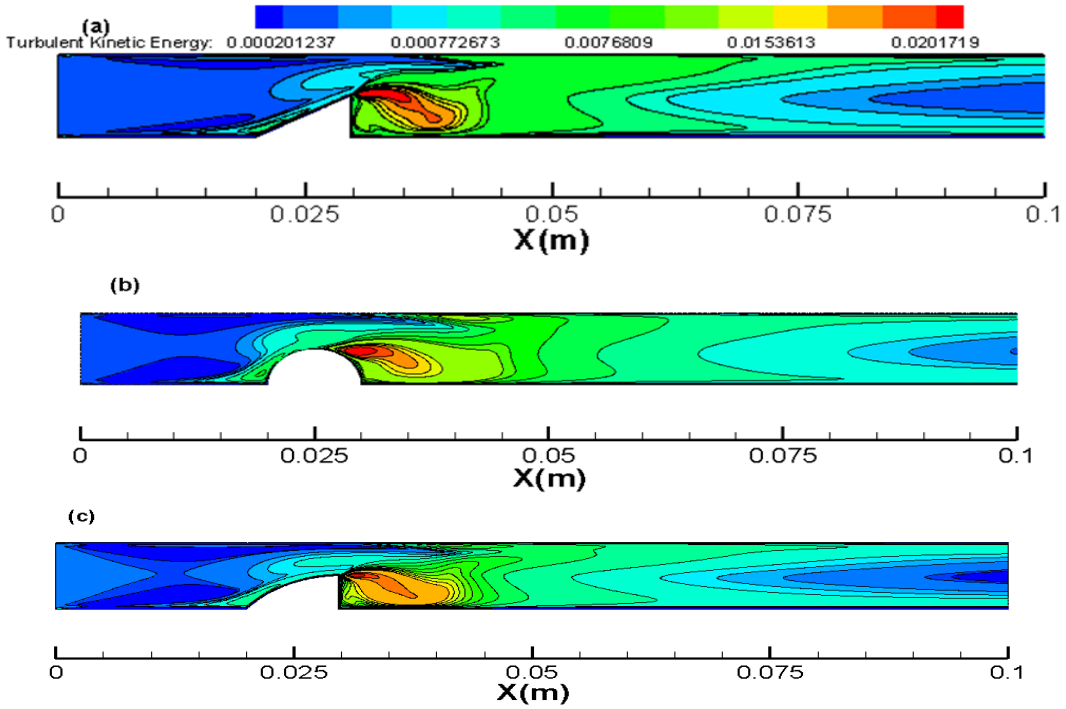

Fig. 6. The turbulent kinetic energy distrubution theough the channal with different vortex chenerator shape (a) triangular VG, (b) Half circle VG, and (c) Quarter circle VG

The effect of installation different VG designs such as triangular, and quarter circle and half circle on the isothermal contour at Reynolds number, which is 5000, step height 5 mm are presented in Figure 7. The overall trend of the flow over the channel agrees with the previous studies on the temperature gradient [10]. From the isothermal contour of the channels, With varied VG shapes, the width of the thermal boundary layer changes. The result demonstrate that different VG design give different fluid flow mixing. The temperature gradient at the wall increases or decrease depending on the VG design and that affect the heat transfer enhancement eventually. That is consistent with the numerical study [26]. It can be observed from the same figure that the quarter VG has a higher temperature gradient followed by half circle and triangular VG shape. The major pattern of the isothermal contour shows the thermal boundary layer decrease after VG step at where X= 0.03 m in the X-direction this point is the starting of the recirculation zone. However, the boundary layer thickness starts to increase again due to the flow developing.

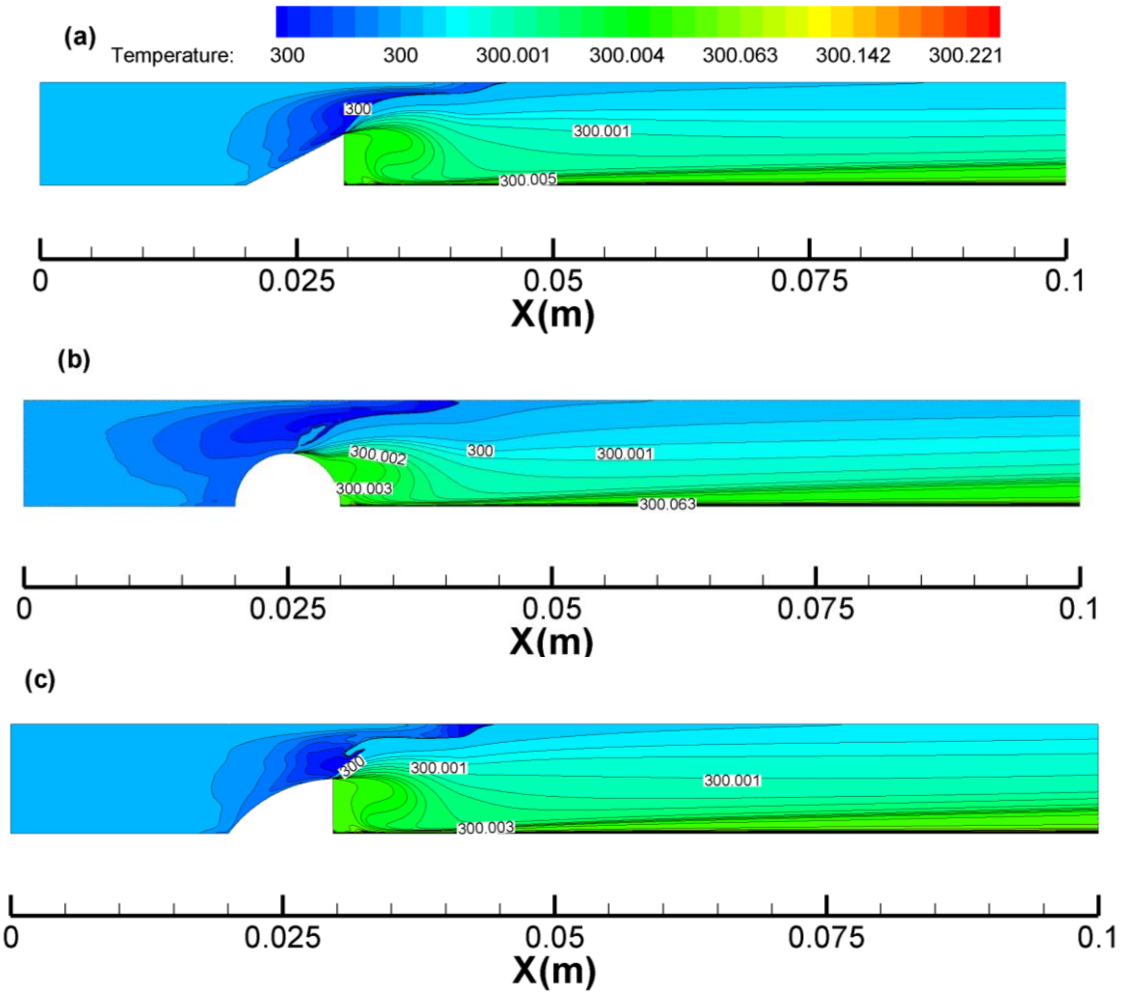

Fig. 7. Effect of different VG design on the isothermal contour (a) triangular VG, (b) Half circle VG, and (c) Quarter circle VG

3.2 Effect of Step Height on Fluid Flow and Heat Transfer

The outcomes of various step height 2, 3, 4, 5, and 6 mm on the surface, The Nu at Re equals 5,000 are seen in Figure 8(a) . The same pattern is found for all step height values checked in this study. The increament in step height had a major impact on the surface Nusselt number Nu increase. This may be attributed to the high-speed gradient after the step of the VG, that rises as height of the

step rises. The surface Nu rose as the step height augmented, according to the data. However, after a step height of 4 mm, the surface Nu reductions, that owing to the decease in the intensity of the recerculation zone after the step. It was observed that step height 4 mm provides the highest surface Nusselt number value among the other step height and that due to the bigger recirculation zone and thinner boundary layer generated because of the step corner. Moreover, Heat transfer enhancement was linked to flow mixing as high as the recirculation region, which resulted in improved heat transfer. Figure 8(b) depicts the local skin friction coefficient at different step heights (2, 3, 4, 5, and 6 mm) and Re = 5,000. When the degree begins to rise, it causes an increase in the values of skin friction, and this is due to the upsurge in the stress of the channel, and thus the upsurge in the degree height leads to a drop in the cross-sectional area. A decrease in the cross section reasons an upsurge in the pressure drop.

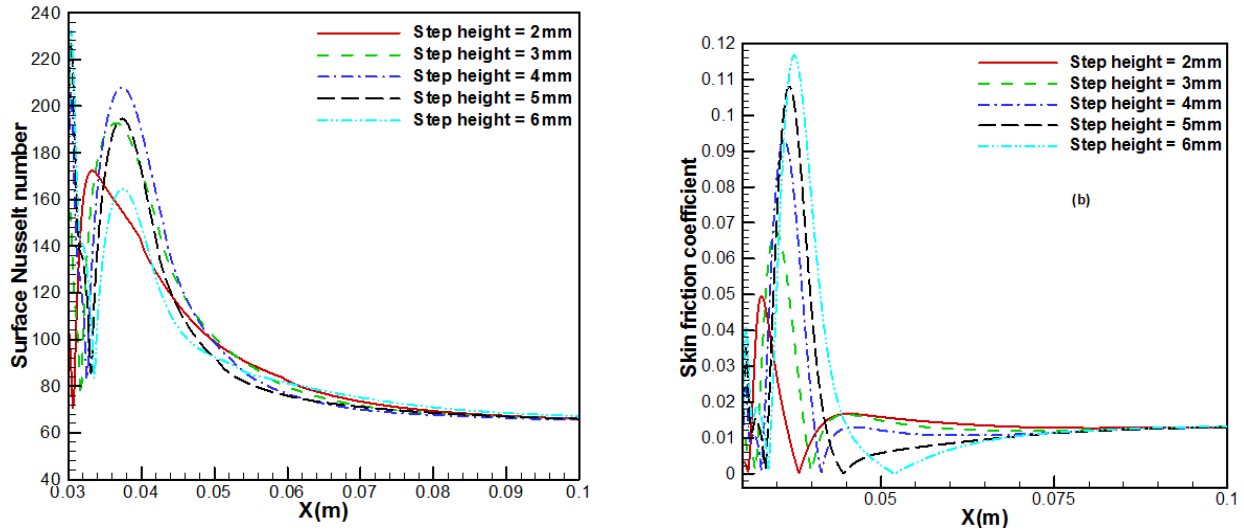

(a) (b)

Fig. 8. The distribution of (a) surface Nusselt number and (b) Skin friction coefficient along the axial direction of the channel at different step height and Re = 5,000

3.3 Effect of Step Height on the Velocity Streamline and Isothermal

Figure 9 the effect was observed in the height of the step on the distribution of the velocity of the flows at Re = 5000, and here the so-called separation zones were created and then the main recycling was done near the step, this is in line with the prior fluid flow results. reported in previous literature [25,26]. The recirculation zone was observed behind the step, and the flow at the edge of the step separated. The velocity streamlines augmented and reduced with the variation in the step height and the maximum velocity behind the step was obtained at step height which is 4 mm. Moreover, the results shows that the size of the separation area of the main recirculation zone was X=0.005 m at step height 2 mm. However, as the step height increases the main separation region increase.

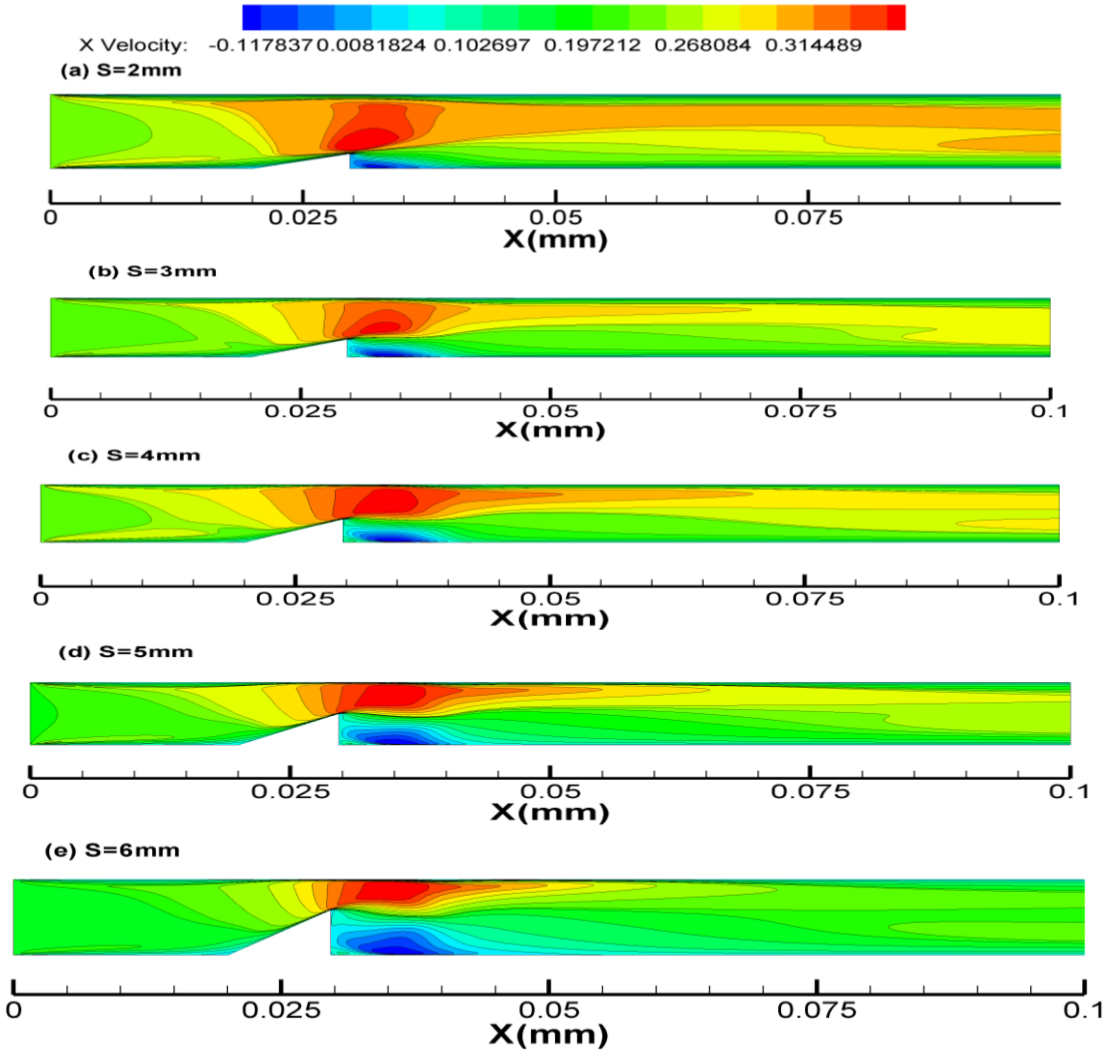

Fig. 9. Simulation results for the velocity streamline over channel with different VG step

Figure 10 depicts the influence of varying step heights (2, 3, 4, 5, and 6 mm) When paired with a VG at Reynolds number 5000, the isothermal contour of the channel is enhanced. The figure shows that the step heights have a noticeable impact on the thermal boundary layer, which rises as the step heights rise. This is due to the increased vortex induced phase portion, which facilitates fluid mixing in the channel. The comes about moreover uncover that there's no substantial advancement within the warm boundary layer after stage tallness of 4 mm, which the ideal liquid blending happens within the channel at a plentifulness stature of 4mm. Besides. As previously said, the warm boundary layer gets to be more slender at X-direction X= 0.03 mm, which is additionally the reattachment.

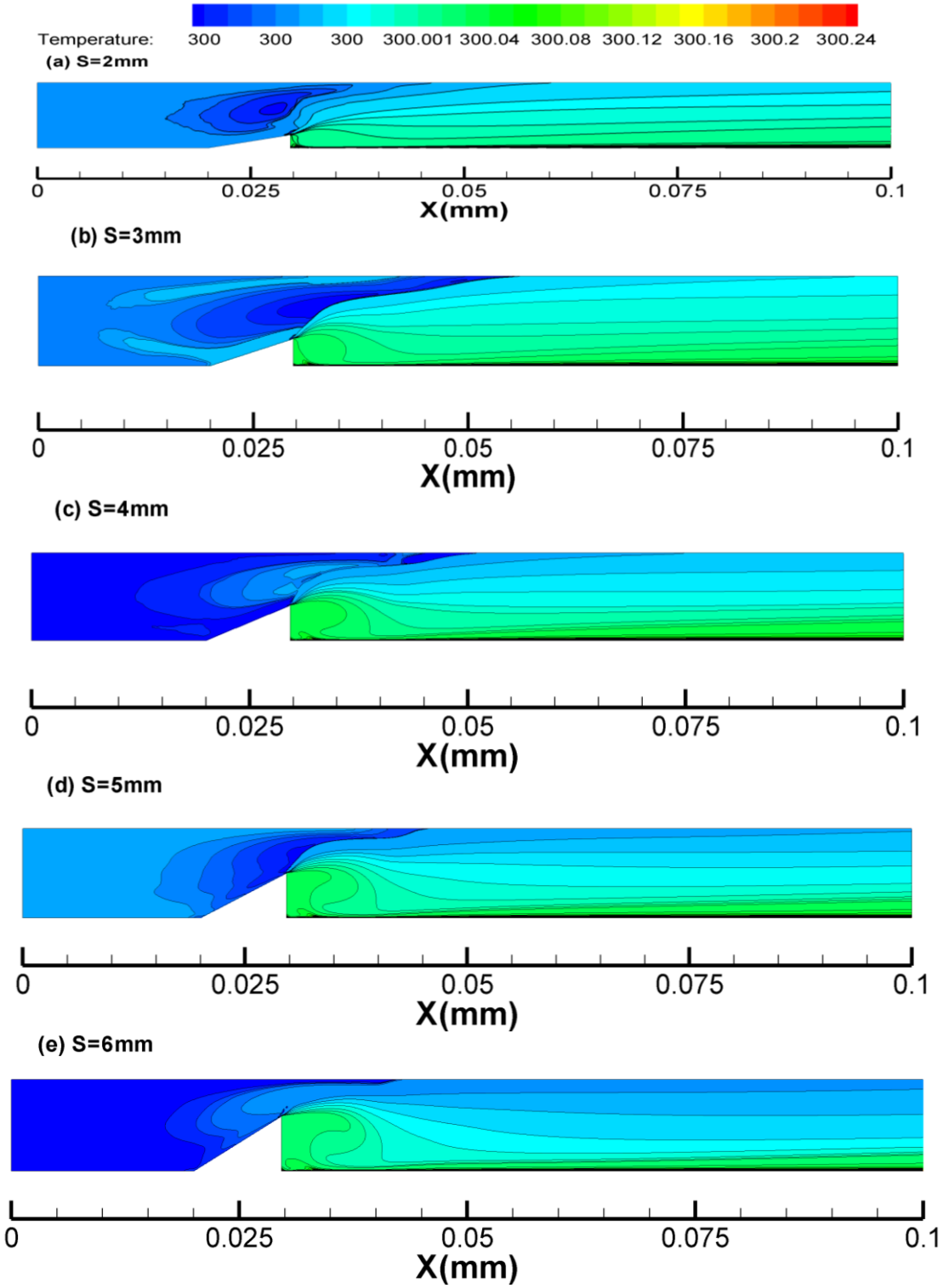

Fig. 10. Effect of Step height of VG on the isothermal contour

3.4 Effect of Reynolds Number on Fluid Flow and Heat Transfer

Figure 11(a) depicts the numerical effects of the average Re with Nu for numerous VG designs. In all three cases, the Nu increases with the flow rate, following a similar pattern. This is due to the VG's high turbulence ability, which causes the wall and the heart to collide quickly. The triangular VG offers the highest advantage in when compared to other layouts, this layout allows for better heat

transmission. This might be because the temperature gradient was increased since the recirculation regime was larger than in the other designs. Figure 11(b) represents all channels for the Re coefficient of skin friction. As the average friction of the skin is inversely associated with the velocity, the overall trend shows a greater skin friction. The value drops at Re = 5,000, and as Re climbed, the value declined. The triangular VG tube had the uppermost average skin friction. The PEC for all numerical cases was determined using equation. Figure 11(c) in comparison to the smooth channel, shows the PEC results for various VG designs. The quarter circular channel has the greatest value of PEC because Nusselt numbers improve more than the friction factor increase. The PEC increases as the Reynolds number upsurges, indicating that the channel with VG is more efficient at high flow rates, according to the findings.

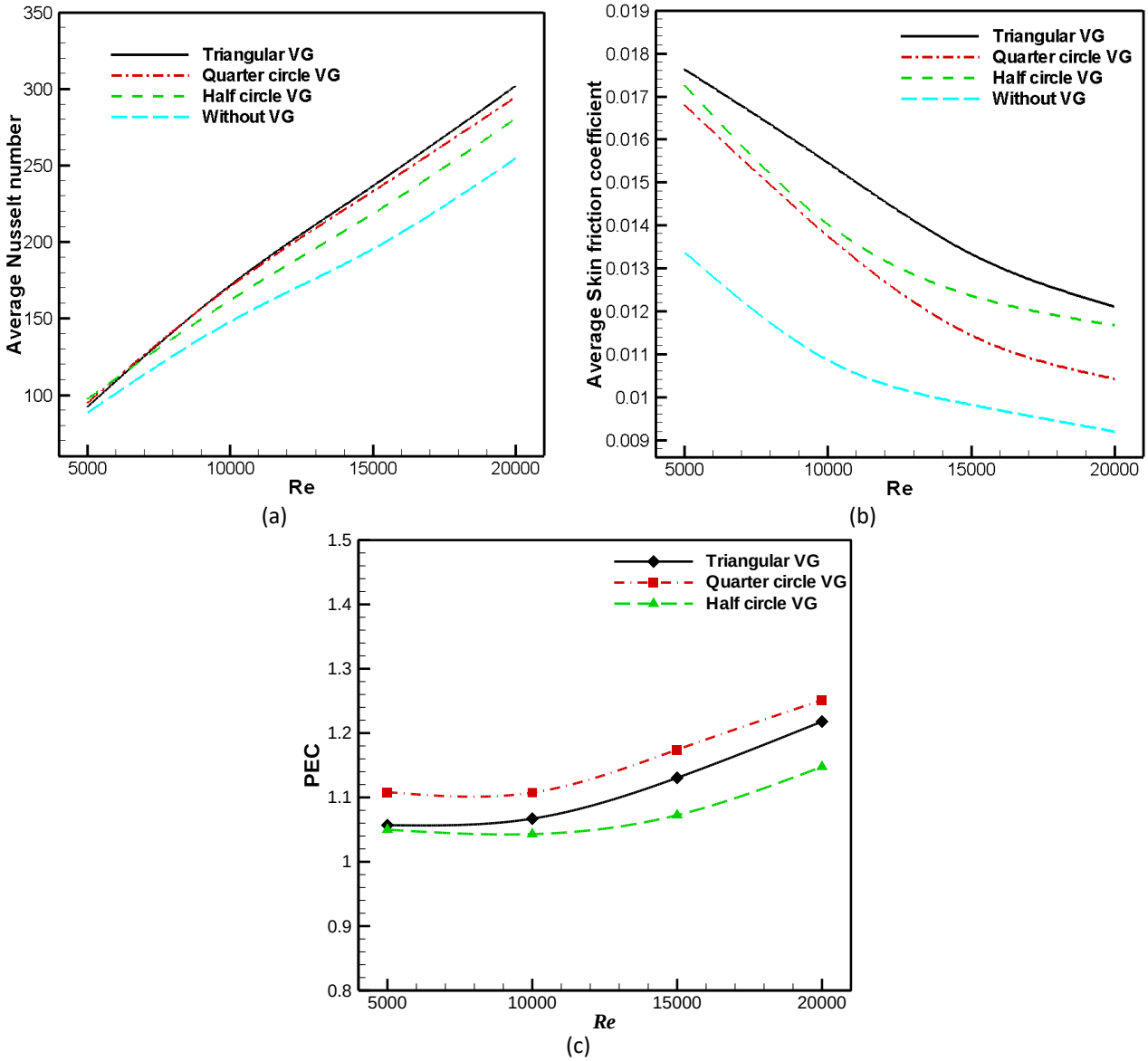

Fig. 11. The PEC with Re for different VG shapes

4. Conclusion

For several years, much work has been expended to improve by adjusting heat exchanger channel design, improve fluid flow and heat transfer features. Channels with VG installation have been

suggested, but none of the studies to date have concentrated on installing various VG designs in the channel to greatly improvement heat transfer, which is the impetus for this study. In this analysis, a numerical review has been carried out using the software program to examine the convective with VG, fluid flow and heat transfer within channel are improved. There are three types of VG models that have been studied: (1) triangular, (2) half circle, and (3) quarter circle. The simulations were run with a Re range of 5,000–20,000, confirming the initial hypothesis. The computational modelling in this study has been done with the software program. The finite volume technique was employed to discretize and resolve the continuity, momentum, and energy equations. To connect the pressure and velocity fields inside the domain, the SIMPLE algorithm scheme has been used. The numerical models of VG channels were developed, validated, and verified against other works in the literature, and the results demonstrated a strong agreement with an error of less than 5%, confirming the second objective.

The effects of geometrical parameters such as step height 2, 3, 4, 5, and 6 mm, as well as Reynolds number Re, there have been presentations and analyses on the flow and thermal fields. Comparisons of the numerical findings with those available in the literature have been presented, and there is a high level of consensus between the results. The Reynolds number ranges from 5,000 to 20,000. By distilled water as the operational fluid.

The skin friction coefficient and the surface Nu rise with step height and reach their maximum value at 4 mm, according to the findings. Furthermore, as the Re increases, so does the average Nu sum. At a step height of 4 mm, the quarter circle VG outperforms the triangular VG in terms of thermal-hydraulic efficiency. The simulation results conform well with those in the literature.

References

[1] Hilo, Ali Kareem, Antonio Acosta Iborra, Mohammed Thariq Hameed Sultan, and Mohd Faisal Abdul Hamid. "Effect of corrugated wall combined with backward-facing step channel on fluid flow and heat transfer." *Energy* 190 (2020): 116294. https://doi.org/10.1016/j.energy.2019.116294

[2] Hilo, Ali, Sadeq Rashid Nfawa, Mohamed Thariq Hameed Sultan, Mohd Faisal Abdul Hamid, and MI Nadiir Bheekhun. "Heat transfer and thermal conductivity enhancement using graphene nanofluid: a review." *Journal of Advanced Research in Fluid Mechanics and Thermal Sciences* 55, no. 1 (2019): 74-87.

[3] Hamid, Mohd Faisal Abdul. "Review of improvements on heat transfer using nanofluids via corrugated facing step." *International Journal of Engineering & Technology* 7, no. 4.13 (2018): 160-169. https://doi.org/10.14419/ijet.v7i4.13.21350

[4] Ajeel, Raheem K., WS-IW Salim, and Khalid Hasnan. "An experimental investigation of thermal-hydraulic performance of silica nanofluid in corrugated channels." *Advanced Powder Technology* 30, no. 10 (2019): 2262-2275. https://doi.org/10.1016/j.apt.2019.07.006

[5] Ajeel, R. K., and W. S. I. W. Salim. "A CFD study on turbulent forced convection flow of Al2O3-water nanofluid in semi-circular corrugated channel." In *IOP Conference Series: Materials Science and Engineering*, vol. 243, no. 1, p. 012020. IOP Publishing, 2017. https://doi.org/10.1088/1757-899X/243/1/012020

[6] Ajeel, Raheem Kadhim, Wan Saiful-Islam Wan Salim, and Khalid Hasnan. "Heat transfer enhancement in semicircle corrugated channel: effect of geometrical parameters and nanofluid." *Journal of Advanced Research in Fluid Mechanics and Thermal Sciences* 53, no. 1 (2019): 82-94.

[7] Hilo, Ali Kareem. "Fluid flow and heat transfer over corrugated backward facing step channel." *Case Studies in Thermal Engineering* 24 (2021): 100862. https://doi.org/10.1016/j.csite.2021.100862

[8] Menni, Younes, Ali J. Chamkha, Ahmed Azzi, and Chafika Zidani. "Numerical analysis of fluid flow and heat transfer characteristics of a new kind of vortex generators by comparison with those of traditional vortex generators." *International Journal of Fluid Mechanics Research* 47, no. 1 (2020). https://doi.org/10.1615/InterJFluidMechRes.2019026753

[9] Salman, Sadeq, Ali Hilo, Sadeq Rashid Nfawa, Mohamed Thariq Hameed Sultan, and Syamimi Saadon. "Numerical Study on the Turbulent Mixed Convective Heat Transfer over 2D Microscale Backward-Facing Step." *CFD Letters* 11, no. 10 (2019): 31-45.

[10] Ajeel, Raheem K., K. Sopian, Rozli Zulkifli, Saba N. Fayyadh, and Ali Kareem Hilo. "Assessment and analysis of binary hybrid nanofluid impact on new configurations for curved-corrugated channel." *Advanced Powder Technology* 32, no. 10 (2021): 3869-3884. https://doi.org/10.1016/j.apt.2021.08.041
[11] Hernon, Domhnaill, and Norah Patten. "Hotwire measurements downstream of a delta winglet pair at two angles of attack." In *Heat Transfer Summer Conference*, vol. 43567, pp. 777-784. 2009. https://doi.org/10.1115/HT2009-88089
[12] Tian, Li-Ting, Ya-Ling He, Yong-Gang Lei, and Wen-Quan Tao. "Numerical study of fluid flow and heat transfer in a flat-plate channel with longitudinal vortex generators by applying field synergy principle analysis." *International Communications in Heat and Mass Transfer* 36, no. 2 (2009): 111-120. https://doi.org/10.1016/j.icheatmasstransfer.2008.10.018
[13] Ferrouillat, Sébastien, Patrice Tochon, C. Garnier, and Hassan Peerhossaini. "Intensification of heat-transfer and mixing in multifunctional heat exchangers by artificially generated streamwise vorticity." *Applied thermal engineering* 26, no. 16 (2006): 1820-1829. https://doi.org/10.1016/j.applthermaleng.2006.02.002
[14] Sanders, Paul A., and Karen A. Thole. "Effects of winglets to augment tube wall heat transfer in louvered fin heat exchangers." *International journal of heat and mass transfer* 49, no. 21-22 (2006): 4058-4069. https://doi.org/10.1016/j.ijheatmasstransfer.2006.03.036
[15] Zhou, Guobing, and Qiuling Ye. "Experimental investigations of thermal and flow characteristics of curved trapezoidal winglet type vortex generators." *Applied Thermal Engineering* 37 (2012): 241-248. https://doi.org/10.1016/j.applthermaleng.2011.11.024
[16] Yoo, Seong-Yeon, Dong-Seong Park, Min-Ho Chung, and Sang-Yun Lee. "Heat transfer enhancement for fin-tube heat exchanger using vortex generators." *KSME international journal* 16, no. 1 (2002): 109-115. https://doi.org/10.1007/BF03185161
[17] Sun, Zhiqiang, Kang Zhang, Wenhao Li, Qiang Chen, and Nianben Zheng. "Investigations of the turbulent thermal-hydraulic performance in circular heat exchanger tubes with multiple rectangular winglet vortex generators." *Applied Thermal Engineering* 168 (2020): 114838. https://doi.org/10.1016/j.applthermaleng.2019.114838
[18] Wang, Jiansheng, Zeyu Sun, and Xueling Liu. "Heat transfer and flow characteristics in a rectangular channel with miniature square column in aligned and staggered arrangements." *International Journal of Thermal Sciences* 155 (2020): 106413. https://doi.org/10.1016/j.ijthermalsci.2020.106413
[19] Althaher, M. A., A. A. Abdul-Rassol, H. E. Ahmed, and H. A. Mohammed. "Turbulent heat transfer enhancement in a triangular duct using delta-winglet vortex generators." *Heat Transfer—Asian Research* 41, no. 1 (2012): 43-62. https://doi.org/10.1002/htj.20382
[20] Ahmed, H. E., H. A. Mohammed, and Mohd Zamri Yusoff. "Heat transfer enhancement of laminar nanofluids flow in a triangular duct using vortex generator." *Superlattices and Microstructures* 52, no. 3 (2012): 398-415. https://doi.org/10.1016/j.spmi.2012.05.023
[21] Carpio, José, and Alvaro Valencia. "Heat transfer enhancement through longitudinal vortex generators in compact heat exchangers with flat tubes." *International Communications in Heat and Mass Transfer* 120 (2021): 105035. https://doi.org/10.1016/j.icheatmasstransfer.2020.105035
[22] Zhang, Guohua, Jian Liu, Bengt Sundén, and Gongnan Xie. "Combined experimental and numerical studies on flow characteristic and heat transfer in ribbed channels with vortex generators of various types and arrangements." *International Journal of Thermal Sciences* 167 (2021): 107036. https://doi.org/10.1016/j.ijthermalsci.2021.107036
[23] Moosavi, Rouhollah, Mehdi Banihashemi, Cheng-Xian Lin, and Po-Ya Abel Chuang. "Combined effects of a microchannel with porous media and transverse vortex generators (TVG) on convective heat transfer performance." *International Journal of Thermal Sciences* 166 (2021): 106961. https://doi.org/10.1016/j.ijthermalsci.2021.106961
[24] Ahmed, Hamdi E., B. H. Salman, and A. Sh Kerbeet. "Heat transfer enhancement of turbulent forced nanofluid flow in a duct using triangular rib." *International Journal of Heat and Mass Transfer* 134 (2019): 30-40. https://doi.org/10.1016/j.ijheatmasstransfer.2018.12.163
[25] Hilo, Ali Kareem, Antonio Acosta Iborra, Mohammed Thariq Hameed Sultan, and Mohd Faisal Abdul Hamid. "Experimental study of nanofluids flow and heat transfer over a backward-facing step channel." *Powder Technology* 372 (2020): 497-505. https://doi.org/10.1016/j.powtec.2020.06.013
[26] Ahmed, M. A., Mohd Zamri Yusoff, Khai Ching Ng, and N. H. Shuaib. "Numerical and experimental investigations on the heat transfer enhancement in corrugated channels using SiO2–water nanofluid." *Case Studies in Thermal Engineering* 6 (2015): 77-92. https://doi.org/10.1016/j.csite.2015.07.003